Available online at www.sciencedirect.com
SCIENCE DIRECT®
International Journal of Pharmaceutics 276 (2004) 115–128
international journal of pharmaceutics
www.elsevier.com/locate/ijpharm

Structural characterisation of water–Tween 40®/Imwitor 308®–isopropyl myristate microemulsions using different experimental methods

F. Podlogar [a], M. Gašperlin [a], M. Tomšič [b], A. Jamnik [b], M. Bešter Rogač [b,*]

[a] *Faculty of Pharmacy, University of Ljubljana, 1000 Ljubljana, Aškerčeva 7, SI, Slovenia*
[b] *Faculty of Chemistry and Chemical Technology, University of Ljubljana, 1000 Ljubljana, Aškerčeva 5, SI, Slovenia*

Received 9 November 2003; received in revised form 11 February 2004; accepted 18 February 2004

Abstract

Pharmaceutically usable microemulsion systems were prepared from water and isopropyl myristate with a constant amount of Tween 40® and Imwitor 308® at a mass ratio of 1. Their type and structure were examined by measuring density and surface tension, and by viscometry, electric conductivity, differential scanning calorimetry (DSC) and small-angle X-ray scattering (SAXS), and the degree of agreement between the techniques was assessed. A model based on monodisperse hard spheres adequately fits the SAXS data in W/O microemulsions predicting, depending on composition, elongated or spherical droplets. It also suggests the involvement of strong attractive interactions in O/W systems. Results of conductivity, viscosity, density and surface tension measurements confirm the prediction of a percolation transition to a bicontinuous structure. DSC detects the degree of water interaction with surfactants thus identifying the type of microemulsion. The conclusions from all the techniques agree well and indicate that such studies could also be carried out on more complex systems. In future, the ability to determine type and structure of such microemulsion systems could enable partitioning and release rates of drugs from microemulsions to be predicted.

Keywords: Microemulsions; SAXS; Viscosity; Surface tension; Density; Conductivity; DSC

1. Introduction

Colloidal drug delivery systems are becoming more and more interesting since they enable the release of drugs to be controlled and/or bioavailability improved. Microemulsions, as dispersions of oil and water, stabilised with a surface active film composed of surfactant and co-surfactant, are of special interest, because of their spontaneous formation, thermodynamic stability and optical transparency (Tenjarla, 1999; Bagwe et al., 2001).

The microemulsion structure is important for the rate of drug release. The wide range of possible structures means that microemulsions can release the solubilised drug at different rates. In an O/W microemulsion, hydrophobic drugs, solubilised mainly in the oil droplets, experience hindered diffusion and are therefore released rather slowly (depending on the oil/water partitioning). The diffusion of water-soluble drugs, on the other hand, is less restrained and they are released rapidly. The reverse behaviour is expected in W/O type. For balanced microemulsions,

* Corresponding author. Tel.: +386-1-2419-410; fax: +386-1-2419-437.
E-mail address: marija.bester@uni-lj.si (M.B. Rogač).

0378-5173/$ – see front matter © 2004 Elsevier B.V. All rights reserved.
doi:10.1016/j.ijpharm.2004.02.018

due to the bicontinous structure, relatively fast diffusion and release occur for both water-soluble and oil-soluble drugs. The structure and composition of microemulsion are highly interrelated, and it is essential to understand this relation in order to control the structure for their more efficient use in both scientific and industrial applications.

In contrast to the easy preparation of microemulsions, however, it is a far from trivial matter to characterise their microstructure. Several authors report that it is possible to determine the state of water in microemulsion system. In most cases a distinction is made between bulk and bound water (Garti et al., 1996, 2000; Garti, 2001; Schulz, 1998; Erzahi et al., 2001). Scattering techniques have been used to characterise the droplet size of the microemulsion (Lang and Glatter, 1996; Kahlweit et al., 1997; Choi et al., 1998; Lipgens et al., 1998; Jakobs et al., 1999; Preu et al., 1999; Hellweg et al., 2000; Svergun et al., 2000; Testard and Zemb, 2000; Endo et al., 2001; Glatter et al., 2001; Mihailescu et al., 2002), however only few with the pharmaceutically acceptable systems (Shukla et al., 2002, 2003; Shukla, 2003). Less attention has been paid to transport properties (Eicke et al., 1989; Boned et al., 1993; D'Aprano et al., 1993; Camett et al., 1995; Giustini et al., 1996; Meier, 1996; Sheu, 1996; Weigert et al., 1997; Testard and Zemb, 2000) and volumetric properties (Lara et al., 1981; Roux-Desngranges et al., 1982; Caron and Desnoyers, 1986; D'Aprano et al., 1993) although they could provide information about the phenomenon of percolation in the system.

A disadvantage of scattering techniques is that, in order to obtain a reliable estimate of droplet size, measurements should be made at a range of low disperse-phase volume fraction in order to avoid the problems encountered as a result of inter-droplet interactions. Many microemulsions of pharmaceutical interest cannot be thus diluted without phase separation.

The aim of this work was to select an appropriate microemulsion system suitable for pharmaceutical use and to use several techniques to determine their type and structure and to monitor the degree of agreement obtained. In this work a pseudo-ternary system water–surfactant (Tween 40®)/co-surfactant (Imwitor 308®)–isopropyl myristate was chosen. The concentration of the surfactant/co-surfactant mixture was kept constant while the ratio of water to oil was varied over a broad range. The potential use of density measurement, viscometry, surface tension measurement, electric conductivity, differential scanning calorimetry (DSC) and small-angle X-ray scattering (SAXS) as experimental methods to characterise the microemulsion system was investigated.

2. Materials and methods

2.1. Materials

Isopropyl myristate (IPM) was obtained from Fluka Chemie GmbH (Switzerland) and used as the lipophilic phase. Tween 40® (TW40)–polyoxyethylene (20) sorbitan monopalmitate (Fluka Chemie GmbH) was used as surfactant and Imwitor® 308 (IMW)–glyceryl caprylate (Condea Chemie GmbH, Germany) as co-surfactant. Twice distilled water was used as hydrophilic phase.

2.2. Preparation of microemulsions

The surfactant and co-surfactant were blended in a 1:1 mass ratio to obtain surfactant mixture. Isopropyl myristate (IPM) was then added and, after brief mixing, the required amount of water was added. Components were blended using a magnetic stirrer for 5 min at room temperature (22 ± 2 °C). The resulting microemulsions were left covered for at least 24 h before further analysis.

The concentration of surfactant mixture was kept constant at 30 wt.% while the ratio of water to IPM was varied between 0 and ∼0.65 weight fraction. The prepared samples represent a line on pseudo-ternary diagram (Fig. 1). Below the chosen line lower concentration of the surfactant mixture does not allow investigation over almost the entire concentration range since microemulsions are not formed. The compositions of the microemulsions investigated are given in Table 1. All of them show stability over 1 year and remain clear and transparent. Samples 0–10 are liquids whereas the last three are gel-like.

2.3. Methods

2.3.1. Density measurements

The density of microemulsions and solvents was measured with a Paar digital precision density meter

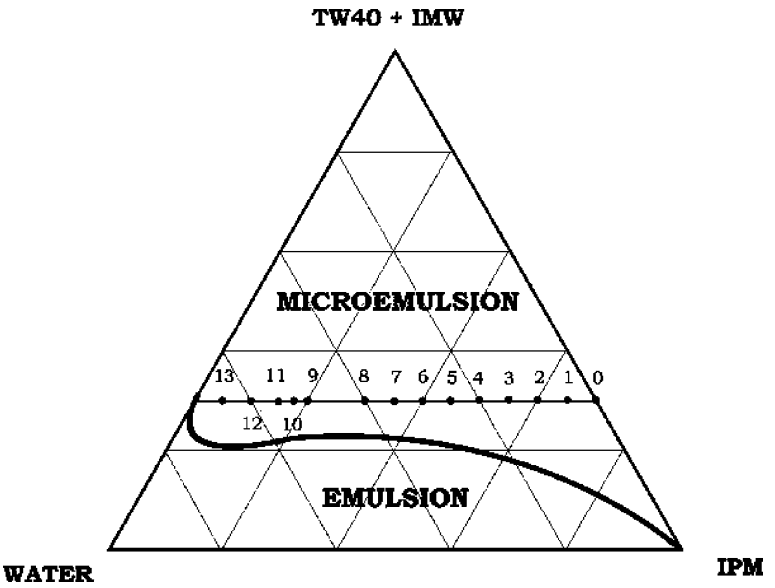

Fig. 1. The pseudo-ternary phase diagram for the mixture isopropyl myristate/Tween 40®/Imwitor 308®/water and the samples chosen for study.

DMA 60 with an external measuring cell DMA 602 (Anton Paar, Graz, Austria). A thermostat controlled the temperature at $25.00 \pm 0.01\,^{\circ}C$. The accuracy of density measurements was within $\pm 5 \times 10^{-6}$ kg/dm.

2.3.2. Surface tension

Surface tension was measured with a Kruss processor tensiometer K21 (Kruss GmbH, Germany) using Wilhelmy's plate method. Measurements were made at $25 \pm 0.5\,^{\circ}C$. A square platinum plate was cleaned, washed off twice with distilled water and heated in a reductive flame to purge all impurities. This cleaning procedure was repeated before every measurement. During the measurement the plate is dipped into the liquid. The tensiometer measures the pulling force of the liquid on the plate and, with known plate size, calculates the surface tension.

Table 1
Composition of the microemulsions studied (see Fig. 1)

Sample	Water (wt.%)	IPM (wt.%)
0	0	70.01
1	5.39	64.71
2	10.01	59.96
3	15.04	54.94
4	20.12	49.73
5	25.01	44.96
6	29.94	39.95
7	35.02	34.95
8	40.05	29.98
9	50.08	19.97
10	52.50	17.48
11	54.92	15.00
12	59.94	10.16
13	65.87	4.85

The concentration of Tween/Imwitor mixture (ratio 1:1) was kept constant at 30 wt.%.

2.3.3. Viscosity

The viscosities of microemulsions were measured with a rotational and oscillatory rheometer Rheolab MC 100 (Paar Physica, Germany), equipped with a cylinder Z3 sensor system. We used the controlled shear rate method at a constant shear rate of 1/*s*. Temperature was controlled at $25 \pm 0.5\,^{\circ}C$.

2.3.4. Electric conductivity measurements

Conductance were measured using a Mettler Toledo MC 226 (Mettler, Switzerland) conductivity meter with a Mettler Toledo Incab® 730 electrode.

2.3.5. DSC

DSC measurements were performed with a differential scanning calorimeter Pyris 1 with Intracooler

2P, both from Perkin-Elmer, USA. Nitrogen with a flow of 20 ml/min was used as purge gas. Approximately 5–15 mg of sample was weighed precisely into a small aluminium pan and quickly sealed hermetically to prevent water evaporation. The empty sealed pan was used as a reference. Samples were cooled from 30 to −60 °C (cooling rate: 10 K/min), held for 3 min at −60 °C and then heated back to 30 °C (heating rate: 10 K/min).

2.3.6. Small-angle X-ray scattering

SAXS experiments were performed with an evacuated Kratky compact camera system (Anton Paar) with a block collimating unit, attached to a conventional X-ray generator (Bruker AXS, Karlsruhe, Germany) equipped with a sealed X-ray tube (Cu-anode target type) producing Ni-filtered Cu Kα X-rays with a wavelength of 0.154 nm. The operating power was 35 kV × 10 mA. The samples were transferred to a standard quartz capillary placed in a thermally controlled sample holder centred in the X-ray beam. The scattering intensities were measured with a linear, position sensitive detector (PSD 50m, M. Braun, Garsching, Germany) detecting the scattering pattern within the whole scattering range simultaneously. All measurements were performed at 25 °C.

For each sample, five SAXS curves with a sampling time between 3600 and 15,000 s were recorded and subsequently averaged to ensure reliable statistics. The absorption of the solutions was determined by using the 'moving slit method' (Stabinger and Kratky, 1978). The smeared data were corrected for experimental broadening by numerical de-smearing with the measured beam cross-section profiles. The result of these calculations is a smooth fit to the smeared data, a de-smeared scattering function, and also the pair-distance distribution function $p(r)$ which is the Fourier transform of the scattering function (Glatter, 1979):

$$I(q) = 4\pi \int_0^\infty p(r) \frac{\sin(qr)}{qr} \, \mathrm{d}r \tag{1}$$

where q is the scattering vector defined as

$$q = \frac{4\pi}{\lambda} \sin\left(\frac{\theta}{2}\right) \tag{2}$$

where λ is the wavelength of X-rays, θ is the scattering angle between the incident beam and the scattered radiation, and r is the distance between two scattering centres within the particle. $p(r)$ was evaluated from the measured $I(q)$ using the indirect Fourier transformation method (program ITP) (Glatter, 1977a,b). For dilute systems with negligible interparticle interactions, it contains information on the size, shape, and inner structure of the scattering objects (Glatter, 1979). At higher concentrations, however, the interactions between the particles partly change the scattering pattern thus giving rise to a deviation of the scattering intensity $I(q)$ from the ideal particle form factor $P(q)$ and consequently to a distortion of the pair-distance distribution function $p(r)$. In reciprocal (q) space, the interparticle interactions are represented by the structure factor $S(q)$, and in real (r) space, by the total correlation function $h(r) = g(r) - 1$ (Hansen and McDonald, 1990), $g(r)$ being the radial distribution function. As the connection between the functions from q and r space (representing the same type of information about the system studied) is the Fourier transformation, $S(q)$ and $h(r)$, like $P(q)$ and $p(r)$, form another Fourier transform pair (Hansen and McDonald, 1990):

$$S(q) - 1 = 4\pi N \int_0^\infty [g(r) - 1] r^2 \frac{\sin(qr)}{qr} \, \mathrm{d}r \tag{3}$$

where N is the particle number density. For systems with no orientation effects, i.e. monodisperse, homogeneous, and isotropic dispersions of spherical particles, the total scattering intensity $I(q)$ can be written as a product of *intra*particle ($P(q)$) and *inter*particle ($S(q)$) contributions:

$$I(q) = NP(q)S(q) \tag{4}$$

When the system is sufficiently dilute, interparticle interactions are significantly reduced, yielding $S(q) = 1$, and ITP evaluation can be used. At higher concentrations the influence of $S(q)$ has to be taken into account. The recently developed technique, a generalised indirect Fourier transformation (GIFT) (Brunner-Popela and Glatter, 1997; Brunner-Popela et al., 1999; Weyerich et al., 1999; Bergmann et al., 2000), allows for the simultaneous determination of both the form factor $P(q)$ and the structure factor $S(q)$. The former remains model free, whereas the latter has to be calculated according to model for interparticle interactions. In the present work, a polydisperse system of hard spheres is chosen as a model, and the Percus–Yevick approximation (Hansen and

McDonald, 1990) is used as the method for calculating $S(q)$. The resulting 'averaged structure factor', averaged over the weighted contributions of partial structure factors for individual monodisperse systems, is determined by three parameters: volume fraction Φ, radius R_{HS} and polydispersity of the hard spheres μ.

3. Results and discussion

One of the main disadvantages of using microemulsions for pharmaceutical use is that they usually contain larger amounts of surfactants. Although this can cause irritation, there is no other way in many cases to obtain stable microemulsion systems. In the system under investigation here, these samples still contain quite a high concentration of surfactant (30 wt.% of Tween/Imwitor). Due to their strong amphiphilic nature they are expected to form a wide variety of different nanostructures dispersed in the continuous phase, which is either oil (IPM) or water, depending on the respective concentrations. In binary systems, spherical micelles are usually formed at low surfactant concentration (above the c.m.c.). On increasing the concentration these micelles grow slightly in size to finally reach the maximal micellar diameter whose value is dictated by the geometrical properties of the surfactant molecules. With further increase of surfactant concentration the micelles start to elongate in one or in two dimensions, leading to their transformation to rod-like particles or bicontinuous and lamellar phases. Because of the high surfactant concentration in the present samples it follows that strong deviations from spherical symmetry are to be expected, especially in the case of pseudo-binary systems where no water (sample 0) is present. In the case of ternary systems, the third component (water or IPM) is captured by the self-organised structures, giving rise to change of shape and/or size. The results of all the methods used confirm this assumption in the microemulsions with low water content.

3.1. Density and surface tension

Values of density and surface tension versus water weight ratio are presented in Fig. 2. Up to 20 wt.% of water the surface tension of the systems does not change greatly. With further increases of water, it first decreases until, at 52 wt.%, a sharp increase is observed. At similar compositions of water, breaking points of the lines in the densities could be observed. The volume of the microemulsion was calculated from the measured density, and the excess volume, $V^E = V_{exp} - V_{id}$, obtained as a function of the water content (Fig. 3). Ideal additivity of volumes of the components: water, isopropyl myristate and surfactant mixture, with densities 0.997047, 0.84965 and 1.05088 g/cm, respectively, was assumed. It is evident

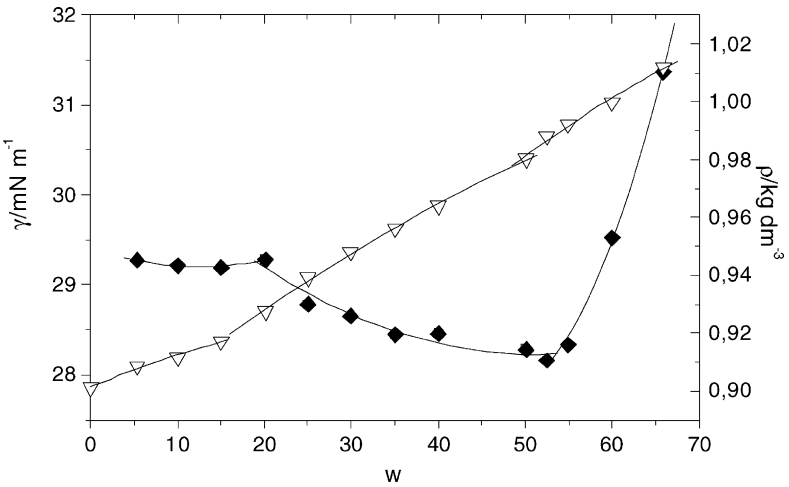

Fig. 2. The variation of surface tension (◆) and density (▽) as a function of water weight ratio (w) in water–Tween 40®/Imwitor 308®–isopropyl myristate microemulsions.

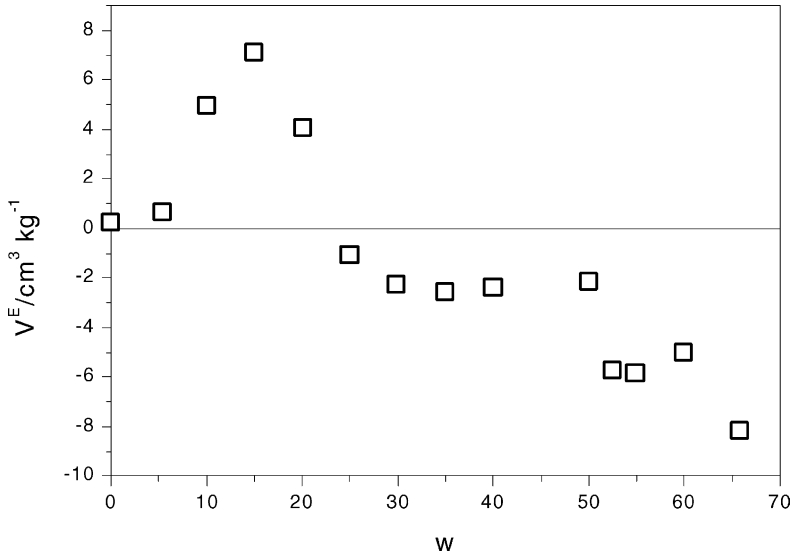

Fig. 3. The excess volume, V^E, of the water–Tween 40®/Imwitor 308®–isopropyl myristate microemulsions as a function of the water content (w).

that, at low content of water the real volume is higher than the ideal volume and that at more than 52 wt.% of water, considerable contraction of volume occurs. Between 25 and 50% of water the volumes are very similar.

The density results were not corrected for the influence of sample viscosity, which could lead up to ∼2% high density values for the last three samples.

3.2. Viscosity and conductivity

Mobility properties expressed with viscosity and electric conductivity are presented in Fig. 4. The viscosity remains almost constant until 52 wt.% water and then increases sharply. A small change occurs in the interval of 25–30 wt.% water (Fig. 4, inset).

The conductivity follows a bell-shaped curve (Fig. 4), as found in microemulsions with fixed surfactant concentration with the percolation transition (Borkovec et al., 1988; Giustini et al., 1996), indicating that the system changes from one of isolated droplets to an interconnected bicontinuous structure.

It has to be pointed out that the occurrence of the percolation transition by electric conductivity measurements for microemulsions with the nonionic surfactants should be studied in the presence of the dissolved electrolyte (Sheu, 1996; Weigert et al., 1997). The added electrolyte provides the charges necessary for the charge transport because the nonionic surfactants do not provide charges to be transported easily along the cluster. In this work the measurements were carried out without added salt since its addition influenced and changed the microemulsion system.

The conductivity of the microemulsions remains around 5 μS/cm in the water rich region and about 1 μS/cm in the oil rich region. Values are much higher than the conductivities of apolar isopropyl myristate (∼0.002 μS/cm) or surfactant mixture (0.5 μS/cm). On the other hand, the microemulsions containing more than 52 wt.% of water exhibit low conductivity which is the result of high viscosity.

The clustering of the droplets at the percolation threshold typically leads to an increase in viscosity (Gradzielski and Hoffman, 1999) and conductivity (Boned et al., 1993; Giustini et al., 1996; Gradzielski and Hoffman, 1999). It has been found that the percolation threshold could be determined from the plot of $(1/\eta)$ $(d\eta/d\Phi)$ versus Φ (Φ: volume fraction of dispersed material). $(1/\eta)$ $(d\eta/dw)$ and specific conductivity, as $(d\kappa/dw)$, are plotted as a function of the water weight fraction (w) (Fig. 5). The maxima of the two plots coincide well at ∼30 wt.% water and confirm the presence of percolative behaviour (Gradzielski and Hoffman, 1999).

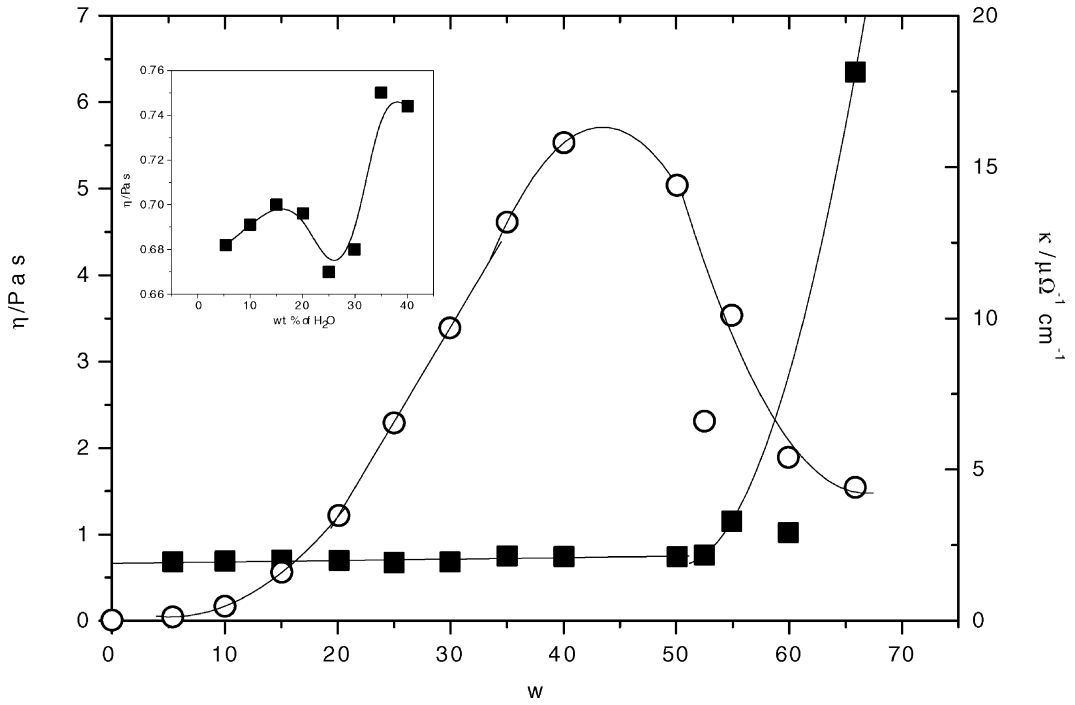

Fig. 4. Electrical conductivity (○) and viscosity (■) as a function of the water weight ratio (w) in the water–Tween 40®/Imwitor 308®–isopropyl myristate microemulsions. *Inset*: Viscosities up to 40 wt.% of water in the system.

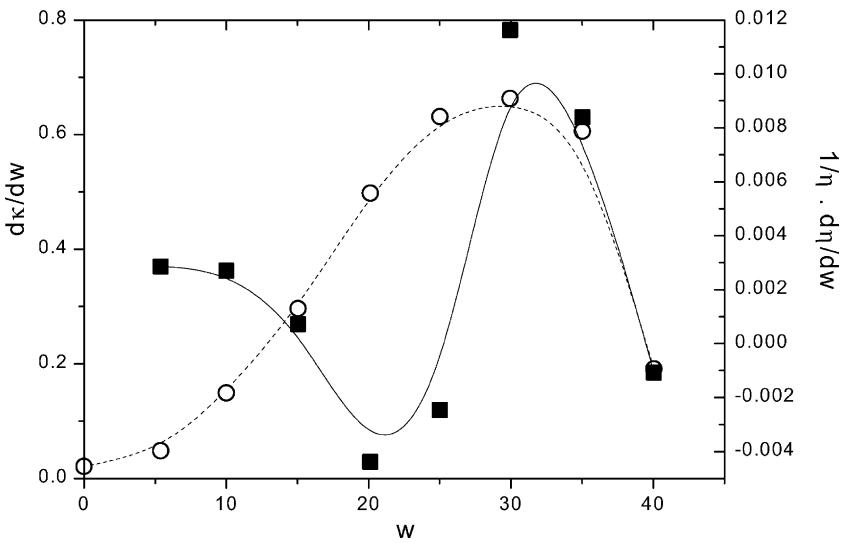

Fig. 5. Plots of $(1/\eta)$ $(d\eta/dw)$ (■) and conductivity change $(d\kappa/dw)$ (○), as a function of the water weight ratio (w) in the water–Tween 40®/Imwitor 308®–isopropyl myristate microemulsions.

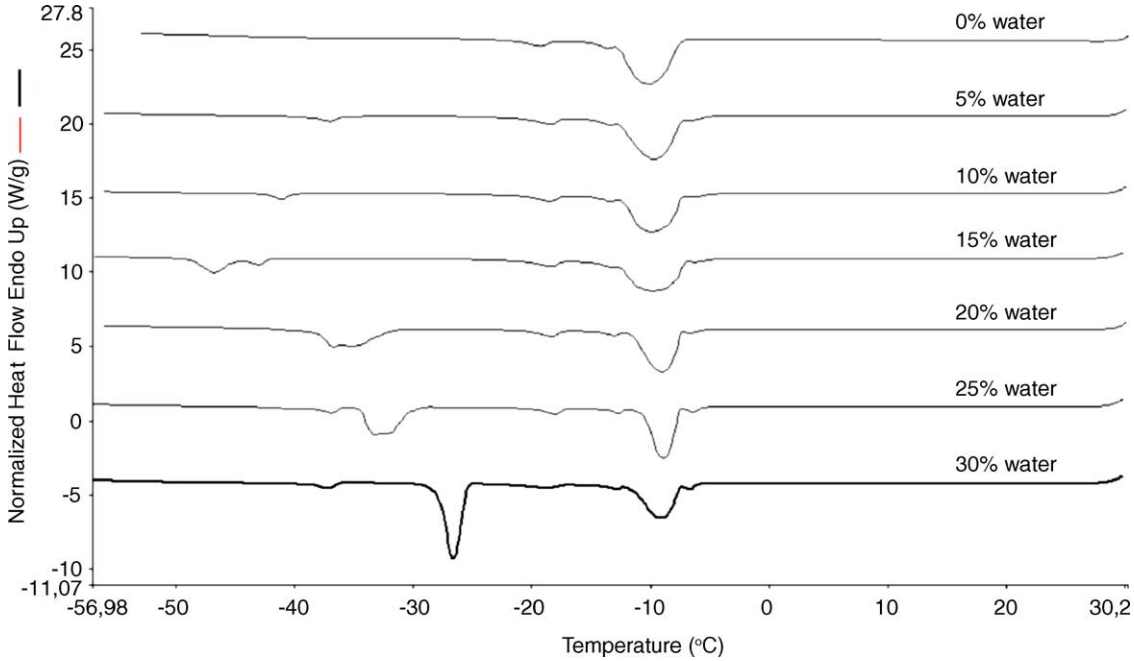

Fig. 6. DSC cooling curves of the microemulsions with less than 30 wt.% of water. The cooling curve for the ternary mixture in the absence of water is also presented.

3.3. DSC measurements

By analysing samples with DSC changes in cooling/heating curve can be observed. For characterisation of our microemulsions the heating part of the curve did not reveal important. So only the cooling curve is presented in this paper. Besides here presented measurement conditions in this paper other temperature programs were also checked with different cooling and/or heating rates, but no additional information was obtained.

In cooling curves of the samples with 5 and 10 wt.% water (Fig. 6), the largest peak appears at approximateky −8 °C and represents solidification of IPM. The second, much smaller peak at approximately −38 °C, probably indicates freezing of surfactant mixture. Although this peak is too small to account for freezing of all the molecules of surfactant and co-surfactant, an additional experiment clearly showed that pure surfactant mixture freezes in that temperature range. In the presence of IPM or water this peak decreases.

A further, very small peak is observed at approximately −18 °C. This peak probably represents solidification of the small amount of IPM impurity (declared purity of used IPM is ≥95%). From Fig. 6, where sample without water also contains that peak, it is clearly seen that the peak cannot represent water in any state.

From 15 to 25 wt.% of water, a distinctive change in the cooling curve is observed (Fig. 6). At 15 wt.% water a new peak appears at approximately −45 °C. With increasing amounts of water, the peak moves towards higher temperatures. Although these peaks are relatively small, it is reasonable to assume that they indicate the freezing of internal or bound water in the system. Since the freezing temperature is very low, the water must be strongly bound or interacts with surfactants.

Pure double distilled water, used as reference in our experiments, shows one large, sharp peak at approximately −17 °C which thus indicates freezing of supercooled water (Milon and Braga, 2003) without any interactions with other molecules (Fig. 7). A similar peak is observed in the temperature range between −17 and −26 °C in samples containing more than 35 wt.% of water (Fig. 7). This peak therefore corresponds to water that is not interacting with other molecules. Nevertheless, some interactions still exist,

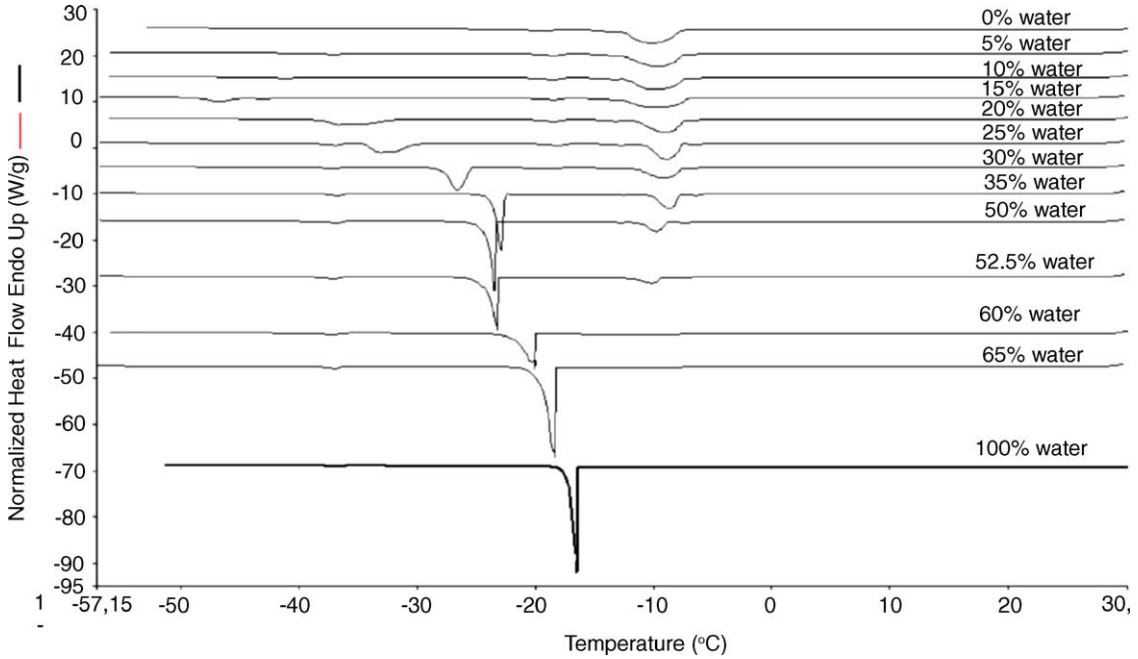

Fig. 7. DSC cooling curves of the microemulsions. Samples without water and pure water alone are also shown.

hence the shift of the freezing temperature towards lower temperatures (compared to pure water) is observed. Lack of presence of the water without interactions present in the systems is expectable, since the investigated microemulsions contain 30 wt.% surfactant mixture and the interactions cannot be neglected. From DSC measurements a conclusion could be made that water in systems containing more than 35 wt.% of it could be in outer phase, thus O/W type of microemulsions is assumed. Still, some of those samples could be also in the intermediate bicontinuous states as in that state water has fewer interactions as in W/O type but still more than in case of pure water. Therefore, it is harder to detect the transition to O/W type of microemulsion where amount of surfactants is high.

3.4. SAXS measurements

The results of SAXS experiments on the Tween/Imwitor/IPM/water system with compositions listed in Table 1 are shown in Fig. 8. In the absence of water, scattering is very weak, owing to the low contrast in electron density of the dispersed scattering objects relative to the continuous phase. The scattering increases markedly with the addition of only a small amount of water and keeps rising with further increases. Specifically, the scattering functions increase considerably and slowly shift towards the lower values of the scattering vector q. The maximum scattering intensity is reached at 25 wt.% of water and then decreases systematically upon further increase of the concentration of water (Fig. 8). In the case of samples with more than 52 wt.% of water a sharp peak develops in the low q region. Sharp peaks are characteristic for the scattering pattern of the lamellar phases, however, the absence of a steep upturn of the scattering intensity at very low q values makes this interpretation unlikely. This sharp peak is most probably, therefore, a pronounced structure factor interaction peak indicating strong interparticle interactions. The SAXS data for samples with 0–15 wt.% of water have been analysed with the GIFT method (Brunner-Popela and Glatter, 1997; Brunner-Popela et al., 1999; Weyerich et al., 1999; Bergmann et al., 2000). This gives the pair-distance distribution function $p(r)$ which provides information about the size and symmetry type of scattering particles, and the structure factor which provides information on interparticle correlations.

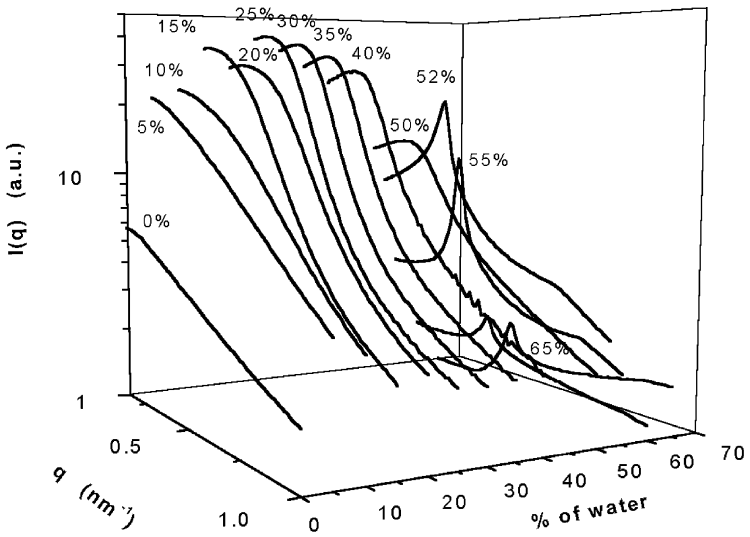

Fig. 8. Scattering curves of the tested samples. Numbers next to the curves correspond to the amount of water.

The number of these parameters and their values are dependent on the model describing the interactions between the particles. Using the polydisperse hard-sphere model coupled with the Percus–Yevick approximation (see Section 2.3.6) the above parameters yield the effective volume fraction Φ, the interaction radius R_{HS} and the polydispersity μ of the hard spheres. Although this model is strictly correct only for uncharged spherical particles, it can also be used for systems that deviate from spherical symmetry (Brunner-Popela et al., 1999; Weyerich et al., 1999; Bergmann et al., 2000). In such cases, however, the interparticle interactions are only approximated and the resulting parameters of the structure factor cannot be trusted quantitatively. It is known that at the very high concentrations of surfactant that cause a high concentration of self-organised scattering structures in the sample, the interparticle interference deviates markedly from the hard sphere type of interactions.

The results of the GIFT evaluation for the samples with 0–15 wt.% of water are shown in Fig. 9. The fits to the experimental SAXS data illustrate the accuracy of the numerical procedure (Fig. 9a). The resulting pair-distance distribution function $p(r)$ is shown in Fig. 9b and the corresponding average structure factor parameters are listed in Table 2. The first $p(r)$ function refers to the pseudo-binary surfactant–co-surfactant/oil sample (sample 0). Its functional form indicates the elongated, rod-like, shape of the micelles with cross-sectional diameter and maximal dimension equal to approximately 5 and 14 nm, respectively. The former value is assessed from the position of the point of inflection between the maximum and the linear region of the $p(r)$ function, whereas the latter is read off from its vanishing point (Glatter and Kratky, 1983; Glatter, 2002). As discussed above, these elongated structures stem from the very high concentration of surfactants (30 wt.%) and would arise from the spherical objects present at lower surfactant concentrations. This object is far from spherical symmetry and consequently, as discussed above, on the limit of capability of the GIFT method. For this reason, this result following from GIFT should be taken with some caution.

The second $p(r)$ function in Fig. 9b indicates that by the adding 5 wt.% of water (sample 1) the shape of the nanostructures changes little, with a slight increase

Table 2
The GIFT parameters of the modelled averaged hard sphere Percus–Yevick structure factor

Sample	Φ (%)	R_{HS} (nm)	μ (%)
0	15.6	12.5	19.60
1	10.9	12.8	16.53
2	5.4	4.8	0.02
3	11.7	7.2	0.25

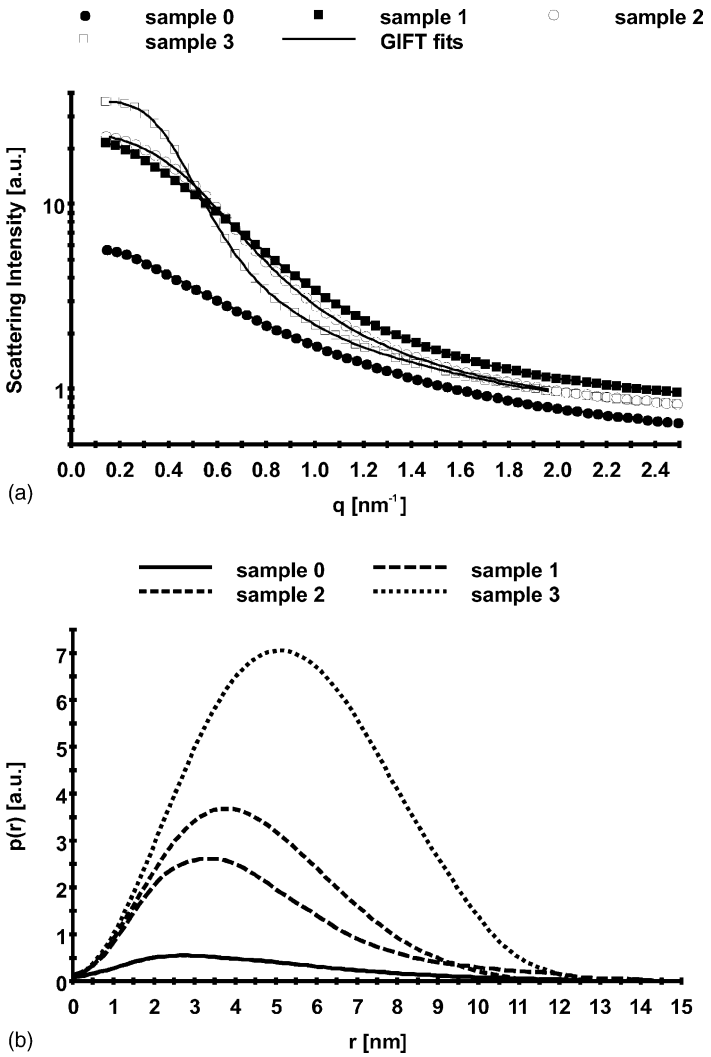

Fig. 9. The results of applying the GIFT evaluation method on the experimental SAXS curves of samples from samples 0 to 3 (see Table 1). (a) Fits of the GIFT evaluation technique to the SAXS curves. (b) The pair-distance distribution functions $p(r)$.

in the length of the rod-like structures up to 15 nm, whereas the scattering contrast increases markedly. Namely, the area under the $p(r)$ function is directly proportional to forward scattering intensity, $I(q = 0)$ (see Eq. (1)). The stronger the contrast the higher also the $I(0)$ which is, in turn, reflected with an increase of this area. In the case of the IPM rich system the Tween molecules are expected to form elongated droplets with their hydrophilic polyoxyethylene moieties oriented towards inside of the droplet. Previous investigations of some other polyoxyethylene based surfactant (Brij 35) systems showed that the polyoxyethylene moiety tends to be strongly hydrated, a feature observed already in the presence of a small amount of water (Tomšič et al., to be published). Accordingly, we expect that also in this case with the oil-rich samples containing some water, the latter will tend to hydrate the polyoxyethylene part of the Tween and hence cooperate in forming the hydrophilic cores. This explains the marked influence of the increasing water amount on the increase of the scattering contrast of these systems, and also confirms the findings

based on the DSC method that the water should be strongly bound in these samples (strong interactions with the hydrophilic groups of the surfactant). The last two curves on Fig. 9b represent the $p(r)$ functions of samples with 10 and 15 wt.% of water. As the amount of water increases, the droplets tend to swell to more spherical structures. This is first accompanied by a slight decrease of the maximal dimension (sample 2) to approximately 12 nm. On further addition of water (sample 3), however, the size of the scattering objects increases slightly to approximately 13 nm. The reason for this is the fact that water enters the core of the droplets and allows that the core dimensions to rise above the limits set by the geometrical properties of the surfactant molecules, as explained above. The $p(r)$ function of sample 3 already has a functional form that is typical of homogeneous globular particles.

The parameters of the averaged structure factor obtained by the GIFT evaluation of the scattering curves are listed in Table 2. According to the mass fractions of the structuring substances (30 wt.% of 1:1 Tween/Imwitor and added water) we could expect the volume fractions Φ to be above 30 wt.%, however they are much lower in all cases. In combination with the finding that the pair-distance distribution functions from Fig. 9b indicate homogeneous structures, which is in clear contradiction to the core-shell droplet structure imposed by the nature of the present surfactants, this could only mean that by SAXS we only see the hydrophilic core of the droplet composed mainly of the polyoxyethylene part of Tween and of water with corresponding overall mass fractions much lower than 30 wt.%. The more hydrophobic Imwitor and the hydrophobic tail of Tween hide in the bulk of the IPM molecules, offering an insufficient scattering contrast to the average electron density in these samples dictated by the IPM. For this reason, this part of the structure cannot be detected by SAXS. In addition, the value of the polydispersity parameter μ is known to be quite high in the case of elongated particles and to be lower in the case of more globular shapes. The findings following from the interpretation of the $p(r)$ functions from Fig. 9b are in agreement with this fact.

In the samples containing moderate water amount the transition to bicontinuous structures and further to oil in water microemulsion is inevitable. This is also the main reason why all of the measured SAXS curves were not evaluated by the GIFT method. It was shown previously that the GIFT evaluation could not be used to determine the transition from the particulate to the bicontinuous structuring (De Campo et al., 2002). According to the results discussed in the previous section we therefore stopped with the GIFT evaluations at sample 3, before the transition to bicontinuous phases could occur.

We also tried to use the GIFT evaluation with the scattering curves of the samples on the water rich side of the phase diagram (samples 11–13), however, no satisfactory fit to the data was achieved. The GIFT procedure could not fit the pronounced peak that developed at low q values. We faced similar problems also in the study of some other systems (Tomšič et al., to be published) in the case of higher surfactant concentrations. According to those findings this peak most probably corresponds to the quite pronounced structure factor interaction peak representing the strong interparticle interactions in these samples that cannot be satisfactorily approximated by the model used here.

4. Conclusions

A polydisperse system of hard spheres has been chosen as a model to interpret the SAXS data, with the following results: the W/O droplets convert from the elongated (rod-like) overall shape of the micelles with cross-section and maximal dimensions equal to approximately 5 and 14 nm, respectively, to more spherical structures which tend to swell with the addition of water. The repulsive interaction results in a positive deviation from the ideal volume.

The SAXS measurements show the presence of strong interparticle interactions between droplets in O/W system. In this region a sharp increase in viscosity and surface tension together with a remarkable diminution of volume was observed. All the results show that the strong attractive forces in the O/W microemulsion effects properties of the system like transformation to gel-like structure. It is expected that the hydrophilic chains of nonionic surfactant are strongly hydrated and connected with hydrogen bonds allowing strong interaction.

Comparing the chosen experimental methods we can conclude that, a microemulsion containing more than approximately 50 wt.% water is expected to be O/W with strongly interacting oil droplets. A

microemulsion containing less than approximately 20 wt.% water is expected to be oil continuous with isolated water droplets, a W/O microemulsion. Finally, a microemulsion containing roughly between 20 and 50 wt.% water will be water as well oil continuous, a bicontinous microemulsions. The data from all methods coincide well and we showed that such studies could be carried also on much more complex pharmaceutically usable microemulsions. In future, the ability to determine type and structure of such microemulsion systems could enable partitioning and release rates of drugs from microemulsions to be predicted.

References

Bagwe, R.P., Kanicky, J.R., Palla, B.J., Patanjali, P.K., Shah, D.O., 2001. Improved drug delivery using microemulsions: rationale, recent progress, and new horizonts. Crit. Rev. Ther. Drug 18, 77–140.

Bergmann, A., Fritz, G., Glatter, O., 2000. Solving the generalized indirect Fourier transformation (GIFT) by Boltzmann simplex simulated annealing (BSSA). J. Appl. Cryst. 33, 1212–1216.

Boned, C., Pyrelasse, J., Saidi, Z., 1993. Dynamic percolation of spheres in a continuum: the case of microemulsions. Phys. Rev. E47, 468–478.

Borkovec, M., Eicke, H.-F., Hammerich, H., Das Gupta, B., 1988. Two percolation processes in microemulsions. J. Phys. Chem. 92, 206–211.

Brunner-Popela, J., Glatter, O., 1997. Small-angle scattering of interacting particles. I. Basic principles of a global evaluation technique. J. Appl. Cryst. 30, 431–442.

Brunner-Popela, J., Mittelbach, R., Strey, R., Schubert, K.V., Kaler, E.W., Glatter, O., 1999. Small-angle scattering of interacting particles. III. D_2O–$C_{12}E_5$ mixtures and microemulsions with *n*-octane. J. Chem. Phys. 110, 10623–10632.

Camett, C., Sciortino, F., Tartaglia, P., Rouch, J., Chen, S.H., 1995. Complex electrical conductivity of water-in-oil microemulsions. Phys. Rev. Lett. 75/3, 569–572.

Caron, G., Desnoyers, J.E., 1986. Study of ternary systems forming stable emulsions. J. Colloid Interface Sci. 119, 114–149.

Choi, S.M., Chen, S.H., Sottman, T., Strey, R., 1998. Measurement of interfacial curvatures in microemulsions using small-angle neutron scattering. Physica B 241–243, 976–978.

D'Aprano, A., D'Arrigo, G., Paparelli, A., Goffredi, M., Liveri, T.V., 1993. Volumetric and transport properties of water/AOT/*n*-heptane microemulsions. J. Phys. Chem. 97, 3614–3618.

De Campo, L., Folmer, B., Leser, M., Glatter, O., 2002. The effect of bicontinuouity in microemulsion systems on small angle scattering data. In: Proceedings of XII International Conference on Small-Angle Scattering, Venice, Italy, August 2002.

Eicke, H.-F., Borkovec, M., Bikram, D.-G., 1989. Conductivity of water-in-oil microemulsions: a quantitative charge fluctuation model. J. Phys. Chem. 93, 314–317.

Endo, H., Mihailecsu, M., Monkenbusch, M., Allgaier, J., Gompper, G., Richter, D., Jakobs, B., Sottman, T., Strey, R., 2001. Effect of amphifilic block copolymers on the structure and phase behaviour of oil–water–surfactant mixtures. J. Chem. Phys. 115, 580–600.

Erzahi, S., Anserin, A., Fanun, M., Garti, N., 2001. Subzero temperature behavior of water in microemulsions. In: Schulz, P.C., Soltero, J.F.A., Puig, J.E. (Eds.), DSC Analysis of Surfactant-Based Microsystems. Thermal Behaviour of Dispersed Systems. Marcel Dekker Inc., New York, pp. 59–181.

Garti, N., Anserin, A., Ezrahi, S., Tiunova, I., Berkovic, B., 1996. Water behaviour in nonionic surfactant systems. I: Subzero temperature behavior of water in nonionic microemulsions studied by DSC. J. Colloid Interface Sci. 178, 60–68.

Garti, N., Anserin, A., Tiunova, I., Fanun, M., 2000. A DSC study of water behavior in water-in-oil microemulsions stabilized by sucrose esters and butanol. Colloid Surface A 170, 1–18.

Garti, N., 2001. Thermal Behavior of Dispersed Systems. Marcel Dekker Inc., New York, pp. 59–181.

Giustini, M., Palazzo, G., Colafemmina, G., DellaMonica, M., Giomini, M., Geglie, A., 1996. Microstructure and dynamics of the water-in-oil CTAB/*n*-pentanol/*n*-hexane/water microemulsion: a spectroscopic and conductivity study. J. Phys. Chem. 70, 959–971.

Glatter, O., 1977a. Data evaluation in small angle scattering: calculation of the radial electron density distribution by means if indirect Fourier transformation. Acta Phys. Austriaca 47, 83–102.

Glatter, O., 1977b. A new method for the evaluation of small-angle scattering data. J. Appl. Cryst. 10, 412–415.

Glatter, O., 1979. The interpretation of real-space information from small-angle scattering techniques. J. Appl. Cryst. 12, 166–175.

Glatter, O., Kratky, O., 1983. Small Angle X-ray Scattering. Academic Press, London.

Glatter, O., Orthaber, D., Stradner, A., Scherf, G., Fanun, M., Garti, N., Clement, V., Leser, E.M., 2001. Sugar–ester nonionic microemulsion: structural characterization. J. Colloid Interface Sci. 241, 215–225.

Glatter, O., 2002. In: Lindner, P., Zemb, Th. (Eds.), Neutrons, X-rays and Light: Scattering Methods Applied to Soft Condensed Matter. Elsevier, Amsterdam.

Gradzielski, M., Hoffman, H., 1999. In: Kumar, P., Mittal, K.L. (Eds.), Rheological Properties of Microemulsions in Handbook of Microemulsion Science and Technology. Marcel Dekker Inc., New York.

Hansen, J.P., McDonald, I.R., 1990. The Theory of Simple Liquids. Academic Press, London.

Hellweg, T., Brulet, A., Sottman, T., 2000. Dynamics in an oil-continous droplet microemulsion as seen by quasielastic scattering techniques. Phys. Chem. Chem. Phys. 2, 5168–5174.

Jakobs, B., Sottman, T., Strey, R., Allgaier, J., Willner, L., Richter, D., 1999. Amphifilic block copolymers as efficiency boosters for microemulsions. Langmuir 15, 6707–6711.

Kahlweit, M., Strey, R., Sottman, T., Busse, G., Faulhaber, B., Jen, J., 1997. Light scattering of oil-in-water globules in nonionic microemulsions. Langmuir 13, 2670–2674.

Lang, P., Glatter, O., 1996. Small-angle X-ray scattering from aquoeus solutions of tetra(oxyethylene)-*n*-octyl ether. Langmuir 12, 1193–1198.

Lara, J., Perron, G., Desnoyers, E., 1981. Heat capacities and volumes of the ternary system benzene–water–2-propanol. J. Phys. Chem. 85, 1600–1605.

Lipgens, S., Schübel, D., Schlicht, L., Spilgies, J.-H., Ilgenfritz, G., 1998. Percolation in nonionic water-in-oil microemulsion systems: a small angle neutron scattering study. Langmuir 14, 1041–1049.

Meier, W., 1996. Poly(oxyethylene) adsorption in water/oil microemulsions: a conductivity study. Langmuir 12, 1188–1192.

Mihailescu, M., Monkenbusch, M., Allgaier, J., Frielinghaus, H., Richter, D., Jakobs, B., Sottmann, T., 2002. Neutron scattering study on the structure and dynamics of oriented lamellar phase microemulsions. Phy. Rev. E 66 (4), art. no. 41504.

Milon, J.J.G., Braga, S.L., 2003. Supercooling water in cylindrical capsules. In: Proceedings of 15th Symposium on Thermophysical Properties, Boulder, CO, USA, June 22–27, 2003.

Preu, H., Zradba, A., Rast, S., Kunz, W., Hardy, E.H., Zeidler, M.D., 1999. Small angle neutron scattering of D_2O–Brij35 and D_2O–alcohol–Brij35 solutions and their modelling using the Percus–Yevick integral equation. Phys. Chem. Chem. Phys. 1, 3321–3329.

Roux-Desngranges, G., Roux, H.A., Groiler, J.-P.E., Viellard, A., 1982. Role of alcohol in microemulsions as determined from volume and heat capacity data for the water–sodium dodecylsulfaet–*n*-butanol system at 255 °C. J. Sol. Chem. 11, 357–375.

Schulz, P.C., 1998. DSC analysis of the state of water in surfactant-based microstructures. J. Thermal Anal. 51, 135–149.

Sheu, Y.E., 1996. Physics of asphaltene micelles and microemulsions—theory and experiment. J. Phys.: Condens. Matter 8, A125–A141.

Shukla, A., Janich, M., Jahn, K., Krause, A., Kiselev, M.A., Neubert, H.H.R., 2002. Investigation of pharmaceutical oil/water microemulsions by small-angle scattering. Pharm. Res. 19/6, 881–886.

Shukla, A., Janich, M., Jahn, K., Neubert, H.H.R., 2003. Microemulsions for dermal drug delivery studied by dynamic light scattering: effect of interparticle interactions in oil-in-water microemulsions. J. Pharm. Sci. 92, 730–738.

Shukla, A., 2003. Characterization of microemulsions using small angle scattering techniques. Dissertation, Martin-Luther-Universität, Halle-Wittenberg, Germany, 2003.

Stabinger, H., Kratky, O., 1978. New technique for measurement of absolute intensity of X-ray small-angle scattering—moving slit method. Makromol. Chem. 179, 1655–1659.

Svergun, D.I., Konarev, P.V., Volkov, V.V., Koch, M.H.J., Sager, W.F.C., Smeets, J., Blokhuis, E.M., 2000. A small angle-X-ray scattering study of the droplet-cylinder transition on oil-rich sodium bis(2-ethylhexyl) sulfsuccinate microemulsions. J. Chem. Phys. 113, 1651–1665.

Tenjarla, S., 1999. Microemulsions: an overview and pharmaceutical applications. Crit. Rev. Ther. Drug 16, 461–521.

Testard, F., Zemb, T., 2000. Solute effect on connectivity of water-in-oil microemulsions. Langmuir 16, 332–339.

Weigert, S., Eicke, H.-F., Meier, W., 1997. Electric conductivity near the percolation transition of a nonionic water-in-oil microemulsion. Physica A 242, 95–103.

Weyerich, B., Brunner-Popela, J., Glatter, O., 1999. Small-angle scattering of interacting particles. II. Generalized indirect Fourier transformation under consideration of the effective structure factor for polydisperse systems. J. Appl. Cryst. 32, 197–209.